Low-Wavenumber Vibrational Dynamics of Liquid Formamide and *N*-Methylformamide: Molecular Dynamics and Instantaneous Normal Mode Analysis

Hajime Torii*

Department of Chemistry, School of Science, The University of Tokyo, Bunkyo-ku, Tokyo 113-0033, Japan

Mitsuo Tasumi

Department of Chemistry, Faculty of Science, Saitama University, Urawa, Saitama 338-8570, Japan

Received: July 27, 1999; In Final Form: October 19, 1999

Low-wavenumber vibrational dynamics are studied for liquid formamide (FA) and *N*-methylformamide (NMF) by the methods of molecular dynamics (MD) and instantaneous normal mode (INM) analysis. The dipole-induced dipole (DID) mechanism is employed for calculating polarizability tensors, the correlation function of which determines Raman spectral profiles and optical Kerr effect (OKE) responses. It is shown that the calculated Raman spectra and OKE responses are in reasonable agreement with those observed in previous studies. The main features of these optical signals are explained by simple librations of the unperturbed molecular polarizability (UMP) tensors, which are considerably anisotropic, although the intensities of the librational components are enhanced to some extent by intermolecular interactions, especially in the case of liquid NMF. The DID term gives rise to smaller intensities in a lower wavenumber region than the UMP term. It is suggested that these features of the optical signals may be regarded as characteristic of strongly interacting liquids with substantial anisotropy in molecular polarizability tensors. It is also shown that the marked difference between the Raman spectra of liquid FA and NMF in the low-wavenumber region arises from a difference in the librations of these molecules around the longer in-plane molecular axis of inertia. The difference is related to the dimensionality of hydrogen bonding in the liquids: two-dimensional in liquid FA and one-dimensional in liquid NMF.

1. Introduction

Low-wavenumber vibrational dynamics of liquids have been extensively studied for the purpose of understanding various properties (time scales, etc.) of the dynamics themselves as well as their role in controlling solvation dynamics and chemical reactions in solution. They have been analyzed in the frequency domain[1,2] by examining far-IR and depolarized Raman (sometimes called "Rayleigh wing" or more simply "light scattering") spectra as well as in the time domain[3−16] by measuring the optical Kerr effect (OKE) or other ultrafast optical responses. It has been discussed[4,6,17−21] that the time dependence of OKE signals and the Fourier transform of far-IR and depolarized Raman spectra may or may not be directly related to the time evolution of solvation dynamics. Because spectral profiles obtained in optical measurements are not the true densities of states of liquid dynamics but contain some factor of light−matter interactions and because each intermolecular vibrational degree of freedom does not contribute equally to solvation dynamics, it is important to understand how the intensities of optical signals are determined and how liquid dynamics control solvation dynamics (and chemical reactions).

In our previous study,[22] the low-wavenumber vibrational spectra and the properties of the modes giving rise to the spectral features have been studied for clusters of formamide (FA) and *N*-methylformamide (NMF), which serve as models of local structures formed in the liquid state, by the ab initio molecular orbital (MO) method. The observed low-wavenumber Raman spectra of liquid FA and NMF[23,24] are known to be different from each other in that strong Raman bands are observed at ∼200 and ∼100 cm^{-1} for liquid FA but only at ∼100 cm^{-1} for liquid NMF. We have shown[22] that strongly Raman-active modes are calculated at ∼200 and ∼100 cm^{-1} for the FA "antiparallel" hexamer (which consists of two antiparallel trimers) but only at ∼100 cm^{-1} for isolated linear clusters of FA and NMF, suggesting that the difference in the observed Raman spectral features arises from the difference in the dimensionality of hydrogen bonding in the liquids (two-dimensional in liquid FA and one-dimensional in liquid NMF). The two-dimensional hydrogen-bonded structure of liquid FA is consistent with the sign and magnitude of the noncoincidence effect observed for the C═O stretching band.[25] We have also shown[22] that the Raman intensities in the low-wavenumber region mainly originate from librational (rotational) motions of molecules in the out-of-plane direction and are explained by the anisotropy of the polarizability tensor of each molecule.

Since the ab initio MO calculations in the above studies were carried out for structures at stationary points, effects of structural disorder characteristic of liquid-state systems were not taken into account. Moreover, effects of anharmonicity inherent in liquid dynamics were not included in the calculations. It is therefore interesting to see how these effects are involved in the Raman spectral features of the liquids.

In the present study, the low-wavenumber Raman spectra of liquid FA and NMF are studied by the methods of molecular

* To whom correspondence should be addressed. Telephone: +81-3-5841-4329. Facsimile: +81-3-3818-4621. E-mail: torii@chem.s.u-tokyo.ac.jp.

10.1021/jp992616k CCC: $19.00
Published on Web 12/03/1999

dynamics (MD) and instantaneous normal mode (INM) analysis.[26,27] The time dependence of the OKE signals is also studied by the MD method. The MD and INM methods are complementary to each other in that MD calculations of Raman spectra are based on long-time correlation functions of polarizability tensors and provide only real wavenumber modes, while INM calculations are useful for analyzing the contributions of translational and librational motions to the densities of states and Raman spectra, although they are based on instantaneous curvatures of the potential energy surface and generate some imaginary wavenumber modes. These calculations are also complementary to our previous ab initio MO calculations in that, in MD and INM calculations, the mechanical properties of the systems (structures, dynamics, and system sizes) are much more realistic, although empirical potential functions are used and some modeling is needed for calculating Raman intensities, while with the MO method, calculations are carried out for much smaller systems but are based on first principles. In the present MD and INM calculations, the dipole-induced dipole (DID) mechanism[28−33] is employed for calculating polarizability tensors. The magnitudes of the Raman and OKE intensities originating from simple librations of anisotropic molecular polarizability tensors and from interaction-induced terms are compared and discussed. The contributions of translational and librational motions to the Raman spectra are also discussed.

2. Computational Procedure

A. MD Simulations. MD simulations were performed on liquid FA and NMF by using the intermolecular potential functions developed by Jorgensen and Swenson[34] in which electrostatic interactions between fixed partial charges and Lennard-Jones interactions are involved. The CH groups in FA and NMF and the methyl group in NMF were treated as united atoms. Only intermolecular degrees of freedom were considered. Four-dimensional vectors (quaternions) were used to represent molecular orientations in solving the equations of motion[35,36] in combination with the leapfrog integration method.[36] Each liquid system consisted of 216 molecules in a cubic cell. The periodic boundary condition was employed. The volume of the cubic cell was fixed so that the molecular volume is equal to 66.8 Å^3 (ref 34) and 98.3 Å^3 (ref 37) for FA and NMF, respectively. The temperature was kept at 298 K by adjusting the total kinetic energy every 400 fs. The time step was set to 2 fs. The system was equilibrated for more than 600 ps, after which a production run of 7.2 ns was carried out.

The depolarized Raman spectrum [$R(\nu)$] and the OKE response signal [$S(t)$] of each liquid system at temperature T were obtained from the time correlation function [$C(t)$] of the anisotropic part of the total polarizability tensor ($\mathbf{\Pi}$) as[1,5,15,38]

$$R(\nu) = \frac{8\pi c}{h}\left[1 - \exp\left(-\frac{hc\nu}{kT}\right)\right] \mathrm{Im} \int_0^\infty \mathrm{d}t \exp(\mathrm{i}2\pi c\nu t)\left[-\frac{\partial}{\partial t}C(t)\right] \quad (1)$$

$$S(t) = -\frac{\theta(t)}{kT}\frac{\partial}{\partial t}C(t) \quad (2)$$

where $\theta(t)$ is the Heaviside step function. $C(t)$ is expressed as

$$C(t) = \sum_{\substack{i,j=x,y,z \\ (i\neq j)}} \langle \Pi_{ij}(t)\, \Pi_{ij}(0)\rangle \quad (3)$$

where $\langle ... \rangle$ denotes the statistical average.

The effective polarizability tensor ($\boldsymbol{\alpha}_p$) of each molecule (numbered by p) in a system was evaluated by the DID mechanism as

$$\boldsymbol{\alpha}_p = \boldsymbol{\alpha}_p^{(0)} + \boldsymbol{\alpha}_p^{(0)} \sum_{\substack{q=1 \\ (q\neq p)}}^{N} \mathbf{T}_{pq}\boldsymbol{\alpha}_q \quad (4)$$

where N is the total number of molecules in the system, $\boldsymbol{\alpha}_p^{(0)}$ is the unperturbed molecular polarizability tensor, and $\mathbf{T}_{pq}$ is the dipole interaction tensor between molecules p and q expressed as

$$\mathbf{T}_{pq} = \frac{3\mathbf{r}_{pq}\mathbf{r}_{pq} - r_{pq}^{\,2}\boldsymbol{I}}{r_{pq}^{\,5}} \quad (5)$$

where $\mathbf{r}_{pq} = \mathbf{r}_p - \mathbf{r}_q$ denotes the distance vector between molecules p and q, r_{pq} is the length of this vector, and $\boldsymbol{I}$ is a 3 × 3 unit tensor. The second term on the right-hand side of eq 4 is the DID term. Since $\boldsymbol{\alpha}_q$ is contained in the DID term, eq 4 should be solved self-consistently. In the present study, the initial estimate of $\boldsymbol{\alpha}_p$ was set equal to $\boldsymbol{\alpha}_p^{(0)}$, and eq 4 was solved iteratively until the difference in $\boldsymbol{\alpha}_p$ between successive iterations was smaller than 10^{-10} Å^3.

In parallel with eq 4, $\mathbf{\Pi}$ is divided into two terms as

$$\mathbf{\Pi} = \mathbf{\Pi}^{\mathrm{UMP}} + \mathbf{\Pi}^{\mathrm{DID}} \quad (6)$$

where

$$\mathbf{\Pi}^{\mathrm{UMP}} = \sum_{p=1}^{N} \boldsymbol{\alpha}_p^{(0)} \quad (7)$$

is the unperturbed molecular polarizability (UMP) term and

$$\mathbf{\Pi}^{\mathrm{DID}} = \sum_{\substack{p,q=1 \\ (p\neq q)}}^{N} \boldsymbol{\alpha}_p^{(0)}\mathbf{T}_{pq}\boldsymbol{\alpha}_q \quad (8)$$

is the DID term. By substitution of eq 6 into eq 3, $C(t)$ is divided into three terms as

$$C(t) = C^{\mathrm{UMP}}(t) + C^{\mathrm{DID}}(t) + C^{\mathrm{U-D}}(t) \quad (9)$$

where the first and second terms are the autocorrelation functions of $\mathbf{\Pi}^{\mathrm{UMP}}$ and $\mathbf{\Pi}^{\mathrm{DID}}$, respectively, and the third term is the cross correlation function between $\mathbf{\Pi}^{\mathrm{UMP}}$ and $\mathbf{\Pi}^{\mathrm{DID}}$. $R(\nu)$ and $S(t)$ are accordingly divided into three terms as

$$R(\nu) = R^{\mathrm{UMP}}(\nu) + R^{\mathrm{DID}}(\nu) + R^{\mathrm{U-D}}(\nu) \quad (10)$$

$$S(t) = S^{\mathrm{UMP}}(t) + S^{\mathrm{DID}}(t) + S^{\mathrm{U-D}}(t) \quad (11)$$

Each term in eqs 10 and 11 is related to the corresponding term in eq 9 in the form given in eqs 1 and 2. $R^{\mathrm{UMP}}(\nu)$ and $S^{\mathrm{UMP}}(t)$ in eqs 11 and 12 are sometimes called "librational" in previous studies, e.g., in ref 39. We do not adopt this notation to distinguish the decomposition in eqs 9−11 from that described below in eq 26 (section 2.B).

All the above calculations were carried out with our original programs on NEC SX-3 and SX-5 supercomputers at the Computer Center of the Institute for Molecular Science.

The unperturbed molecular polarizability tensors [$\boldsymbol{\alpha}_p^{(0)}$] of FA and NMF were calculated by the ab initio molecular orbital

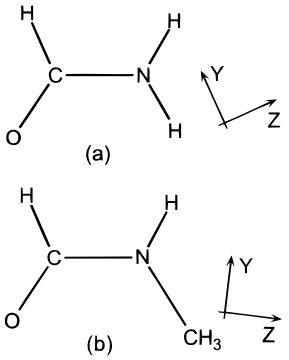

Figure 1. Principal axes of inertia of (a) formamide and (b) *N*-methylformamide.

(MO) method at the Hartree−Fock level. The 6-31(+)G** basis set (the 6-31G** basis set augmented by one set of diffuse functions on each of the oxygen and nitrogen atoms) was used. The ab initio MO calculations were performed with the Gaussian 94 program[40] on SP2 computers at the Computer Center of the Institute for Molecular Science.

B. INM Analyses. INMs were calculated for 100 configurations of each liquid system taken from the MD simulations described in section 2.A. For calculating INMs, force constant matrices (**F** matrices) with respect to intermolecular vibrational degrees of freedom were constructed. We defined three translational and three librational (rotational) coordinates for each molecule on the basis of its principal axes of inertia. As shown in Figure 1 (in the same way as in our previous study[22]), the *x* axis was defined to be the out-of-plane axis and the *y* and *z* axes were the shorter and longer in-plane axes, respectively. Each of the above coordinates was weighted by a factor determined by atomic masses so that it is related to INMs and mass-weighted Cartesian coordinates (Cartesian coordinates weighted by the square root of atomic masses) by orthogonal transformations. Thus, INMs were obtained by diagonalization of the **F** matrices constructed in this coordinate system. For each configuration, there were three modes with zero eigenvalues that correspond to overall translation of the system. The other $6N - 3$ modes had nonzero eigenvalues.

The polarizability derivatives with respect to translational coordinates (u_{kq}; $k = x, y, z$; $1 \le q \le N$) are expressed as

$$\frac{\partial \boldsymbol{\alpha}_p}{\partial u_{kq}} = \boldsymbol{\alpha}_p^{(0)} \sum_{\substack{r=1 \\ (r \neq p)}}^{N} \frac{\partial \mathbf{T}_{pr}}{\partial u_{kq}} \boldsymbol{\alpha}_r + \boldsymbol{\alpha}_p^{(0)} \sum_{\substack{r=1 \\ (r \neq p)}}^{N} \mathbf{T}_{pr} \frac{\partial \boldsymbol{\alpha}_r}{\partial u_{kq}} \tag{12}$$

Both terms on the right-hand side of this equation originate from the DID term of eq 4 because $\boldsymbol{\alpha}_p^{(0)}$ is independent of u_{kq}. The first term was calculated by using the solution for $\boldsymbol{\alpha}_r$ obtained in eq 4. Since $\partial \boldsymbol{\alpha}_r / \partial u_{kq}$ is contained in the second term, eq 12 was solved iteratively until the difference in $\partial \boldsymbol{\alpha}_p / \partial u_{kq}$ between successive iterations was smaller than 10^{-10} Å^2.[41] The sum over p of eq 12, we obtain

$$\frac{\partial \boldsymbol{\Pi}^{\mathrm{UMP}}}{\partial u_{kq}} = 0 \tag{13}$$

$$\frac{\partial \boldsymbol{\Pi}^{\mathrm{DID}}}{\partial u_{kq}} = \sum_{\substack{p,r=1 \\ (p \neq r)}}^{N} \boldsymbol{\alpha}_p^{(0)} \left(\frac{\partial \mathbf{T}_{pr}}{\partial u_{kq}} \boldsymbol{\alpha}_r + \mathbf{T}_{pr} \frac{\partial \boldsymbol{\alpha}_r}{\partial u_{kq}} \right) \tag{14}$$

The polarizability derivatives with respect to librational coordinates (w_{kq}; $k = x, y, z$; $1 \le q \le N$) are expressed as

$$\frac{\partial \boldsymbol{\alpha}_p}{\partial w_{kq}} = \delta_{pq} \frac{\partial \boldsymbol{\alpha}_p^{(0)}}{\partial w_{kp}} + \delta_{pq} \frac{\partial \boldsymbol{\alpha}_p^{(0)}}{\partial w_{kp}} \sum_{\substack{r=1 \\ (r \neq p)}}^{N} \mathbf{T}_{pr} \boldsymbol{\alpha}_r + \boldsymbol{\alpha}_p^{(0)} \sum_{\substack{r=1 \\ (r \neq p)}}^{N} \mathbf{T}_{pr} \frac{\partial \boldsymbol{\alpha}_r}{\partial w_{kq}} \tag{15}$$

considering that $\mathbf{T}_{pr}$ is independent of w_{kq}. The first term on the right-hand side of this equation originates from the UMP term of eq 4. The second and third terms are the DID terms. This equation was also solved iteratively until the difference in $\partial \boldsymbol{\alpha}_p / \partial w_{kq}$ between successive iterations was smaller than 10^{-10} Å^2 amu$^{-1/2}$. Taking the sum over p of eq 15, we obtain

$$\frac{\partial \boldsymbol{\Pi}^{\mathrm{UMP}}}{\partial w_{kq}} = \frac{\partial \boldsymbol{\alpha}_q^{(0)}}{\partial w_{kq}} \tag{16}$$

$$\frac{\partial \boldsymbol{\Pi}^{\mathrm{DID}}}{\partial w_{kq}} = \sum_{\substack{r=1 \\ (r \neq q)}}^{N} \frac{\partial \boldsymbol{\alpha}_q^{(0)}}{\partial w_{kq}} \mathbf{T}_{qr} \boldsymbol{\alpha}_r + \sum_{\substack{p,r=1 \\ (p \neq r)}}^{N} \boldsymbol{\alpha}_p^{(0)} \mathbf{T}_{pr} \frac{\partial \boldsymbol{\alpha}_r}{\partial w_{kq}} \tag{17}$$

The polarizability derivatives with respect to INMs (Q_n; $1 \le n \le 6N$) are expressed as

$$\frac{\partial \boldsymbol{\Pi}^{\mathrm{UMP}}}{\partial Q_n} = \sum_{q=1}^{N} \sum_{k=x,y,z} \frac{\partial \boldsymbol{\Pi}^{\mathrm{UMP}}}{\partial w_{kq}} \frac{\partial w_{kq}}{\partial Q_n} \tag{18}$$

$$\frac{\partial \boldsymbol{\Pi}^{\mathrm{DID}}}{\partial Q_n} = \sum_{q=1}^{N} \sum_{k=x,y,z} \left(\frac{\partial \boldsymbol{\Pi}^{\mathrm{DID}}}{\partial u_{kq}} \frac{\partial u_{kq}}{\partial Q_n} + \frac{\partial \boldsymbol{\Pi}^{\mathrm{DID}}}{\partial w_{kq}} \frac{\partial w_{kq}}{\partial Q_n} \right) \tag{19}$$

where $\partial u_{kq} / \partial Q_n$ and $\partial w_{kq} / \partial Q_n$ are elements of the eigenvectors of the **F** matrix. The depolarized Raman spectra were calculated by using the off-diagonal elements of the polarizability derivatives as[1,42,43]

$$R^{\mathrm{UMP}}(\nu) = \sum_{n=1}^{6N} \delta(\nu - \nu_n) \sum_{\substack{i,j=x,y,z \\ (i \neq j)}} \left(\frac{\partial \Pi_{ij}^{\mathrm{UMP}}}{\partial Q_n} \right)^2 \tag{20}$$

$$R^{\mathrm{DID}}(\nu) = \sum_{n=1}^{6N} \delta(\nu - \nu_n) \sum_{\substack{i,j=x,y,z \\ (i \neq j)}} \left(\frac{\partial \Pi_{ij}^{\mathrm{DID}}}{\partial Q_n} \right)^2 \tag{21}$$

$$R^{\mathrm{U-D}}(\nu) = 2 \sum_{n=1}^{6N} \delta(\nu - \nu_n) \sum_{\substack{i,j=x,y,z \\ (i \neq j)}} \frac{\partial \Pi_{ij}^{\mathrm{UMP}}}{\partial Q_n} \frac{\partial \Pi_{ij}^{\mathrm{DID}}}{\partial Q_n} \tag{22}$$

where ν_n is the wavenumber (in units of cm^{-1}) of the nth mode given as

$$\nu_n = 1302.791\, \lambda_n^{1/2} \tag{23}$$

where λ_n is the nth eigenvalue (in units of mdyn Å^{-1} amu^{-1}) of the **F** matrix.

The polarizability derivatives are decomposed in eqs 18 and 19 according to the origin of the polarizability, the first and second terms in eq 4. Alternatively, they may be decomposed according to the nature of the eigenvectors ($\partial u_{kq} / \partial Q_n$ and $\partial w_{kq} /$

∂Q_n) into the translational and librational contributions as

$$\frac{\partial \boldsymbol{\Pi}^{\mathrm{trans}}}{\partial Q_n} = \sum_{q=1}^{N} \sum_{k=x,y,z} \frac{\partial \boldsymbol{\Pi}^{\mathrm{DID}}}{\partial u_{kq}} \frac{\partial u_{kq}}{\partial Q_n} \tag{24}$$

$$\frac{\partial \boldsymbol{\Pi}^{\mathrm{lib}}}{\partial Q_n} = \sum_{q=1}^{N} \sum_{k=x,y,z} \left(\frac{\partial \boldsymbol{\Pi}^{\mathrm{UMP}}}{\partial w_{kq}} + \frac{\partial \boldsymbol{\Pi}^{\mathrm{DID}}}{\partial w_{kq}} \right) \frac{\partial w_{kq}}{\partial Q_n} \tag{25}$$

The Raman spectra are accordingly decomposed into three terms as

$$R(\nu) = R^{\mathrm{trans}}(\nu) + R^{\mathrm{lib}}(\nu) + R^{\mathrm{t-l}}(\nu) \tag{26}$$

where

$$R^{\mathrm{trans}}(\nu) = \sum_{n=1}^{6N} \delta(\nu - \nu_n) \sum_{\substack{i,j=x,y,z \\ (i \neq j)}} \left(\frac{\partial \Pi_{ij}^{\mathrm{trans}}}{\partial Q_n} \right)^2 \tag{27}$$

$$R^{\mathrm{lib}}(\nu) = \sum_{n=1}^{6N} \delta(\nu - \nu_n) \sum_{\substack{i,j=x,y,z \\ (i \neq j)}} \left(\frac{\partial \Pi_{ij}^{\mathrm{lib}}}{\partial Q_n} \right)^2 \tag{28}$$

$$R^{t-l}(\nu) = 2 \sum_{n=1}^{6N} \delta(\nu - \nu_n) \sum_{\substack{i,j=x,y,z \\ (i \neq j)}} \frac{\partial \Pi_{ij}^{\mathrm{trans}}}{\partial Q_n} \frac{\partial \Pi_{ij}^{\mathrm{lib}}}{\partial Q_n} \tag{29}$$

Note that $R^{\mathrm{lib}}(\nu)$ includes the effect of $\partial \boldsymbol{\Pi}^{\mathrm{DID}}/\partial w_{kq}$, in contrast to $R^{\mathrm{UMP}}(\nu)$ in eq 20.

All the calculations described in this section were carried out with our original programs on NEC SX-3 and SX-5 supercomputers at the Computer Center of the Institute for Molecular Science.

3. Results and Discussion

A. MD Simulations of Raman Spectra and OKE Responses. The Raman spectra of liquid FA and NMF obtained from MD simulations by using eqs 1 and 3 are shown in Figure 2. It is noted that the wavenumber region with strong Raman intensities extends from ~100 to over 200 cm^{-1} in the case of liquid FA, while it is limited to a much narrower range (around 130 cm^{-1}) in the case of liquid NMF. This result is consistent with the observed Raman spectral features of these two liquids,[23,24] suggesting that the main factors giving rise to the difference in the spectral features between the two liquids are involved in the present calculations. It is also consistent with the results of the ab initio MO calculations carried out for clusters of FA and NMF in our previous study.[22] It may be said that the most prominent difference in the Raman spectral features between the two liquids is related to the difference in the local liquid dynamics, the properties of which do not change very much by the effects of anharmonicity and structural disorder.

Each of the Raman spectra shown in Figure 2 is decomposed into three terms according to eq 10. It is seen that the UMP term [$R^{\mathrm{UMP}}(\nu)$] dominates the whole wavenumber range, especially in the case of liquid FA. This result indicates that the anisotropy of the unperturbed molecular polarizability tensor [$\boldsymbol{\alpha}_p^{(0)}$] is large enough in comparison with the contribution of the DID term of $\boldsymbol{\alpha}_p$ so that the time derivative of $C(t)$ arising from simple librations of $\boldsymbol{\alpha}_p^{(0)}$ explains the main part of the Raman intensities in the wavenumber region examined in this

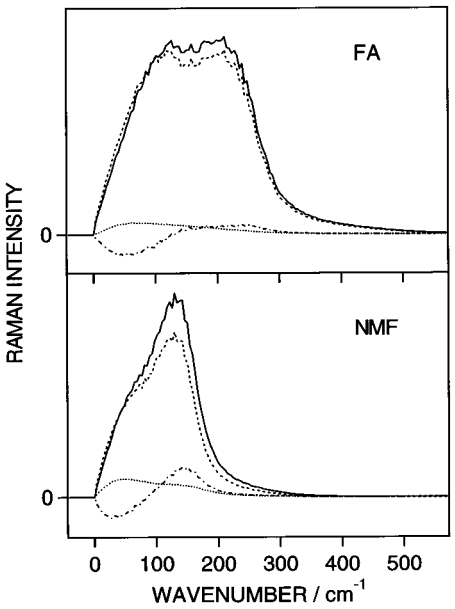

Figure 2. Raman spectra of liquid formamide (FA) and *N*-methylformamide (NMF) calculated by the MD method: (solid line) total profile; (dashed line) unperturbed molecular polarizability (UMP) component; (dotted line) dipole-induced dipole (DID) component; (dot−dashed line) UMP−DID cross term. Intensities are given on an arbitrary scale.

study. The DID term [$R^{\mathrm{DID}}(\nu)$] gives rise to some intensities in the 0−100 cm^{-1} region, but they are canceled by the contribution of the cross term [$R^{\mathrm{U-D}}(\nu)$]. The result that the contribution of the DID term appears in a wavenumber region lower than that of the UMP term is in contrast to that obtained for liquid carbon disulfide[33,39,44,45] and liquid acetonitrile,[46] indicating that this spectral feature may be regarded as characteristic of strongly interacting (e.g., hydrogen-bonding) liquids. The cross term gives rise to positive Raman intensities in the region above 100 cm^{-1}, especially in the case of liquid NMF. It may be said that this term redistributes some intensities from the 0−100 cm^{-1} region to the 100−200 cm^{-1} region. A similar spectral pattern of the cross term has also been seen for liquid acetonitrile.[19]

As explained above, in order that the UMP term [$R^{\mathrm{UMP}}(\nu)$] dominates the Raman spectra, the contribution of the DID term of $\boldsymbol{\alpha}_p$ should be sufficiently small. For example, the UMP−DID cross term [$R^{\mathrm{U-D}}(\nu)$] is important in the Raman spectra of liquid carbon disulfide,[39] although the anisotropy in $\boldsymbol{\alpha}_p^{(0)}$ of a carbon disulfide molecule is regarded to be very large. To the lowest order in $\boldsymbol{\alpha}_p^{(0)}$, the magnitude of the DID term of $\boldsymbol{\alpha}_p$ (eq 4) scales as the square of $\boldsymbol{\alpha}_p^{(0)}$ divided by the cube of intermolecular distances. The large magnitude of $R^{\mathrm{U-D}}(\nu)$ in the Raman spectra of liquid carbon disulfide[39] (compared with the cases of liquid FA and NMF treated in the present study) may originate from the large value of the isotropic polarizability, expressed as $\mathrm{Tr}[\boldsymbol{\alpha}_p^{(0)}]/3$ and from the substantially nonspherical shape of the molecule, resulting in short intermolecular distances between neighboring molecules located side by side.

The OKE responses of liquid FA and NMF calculated by using eqs 2 and 3 are shown in Figure 3. They are in good agreement with the experimental results obtained by Chang and Castner,[8,9] indicating that the short-time liquid dynamics obtained from the present MD simulations are reasonable and that an appropriate intensity-generating mechanism is adopted in the calculations.

As expected from the results for the Raman spectra described above, the oscillatory profiles of the OKE responses are mainly explained by the contribution of the UMP term [$S^{\mathrm{UMP}}(t)$ in eq

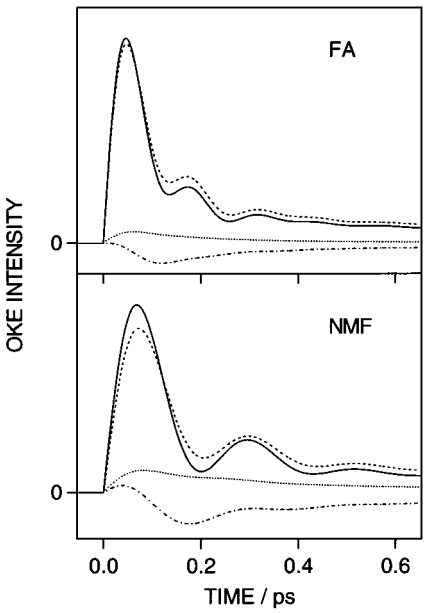

Figure 3. Optical Kerr effect responses of liquid formamide (FA) and *N*-methylformamide (NMF) calculated by the MD method: (solid line) total profile; (dashed line) unperturbed molecular polarizability (UMP) component; (dotted line) dipole-induced dipole (DID) component; (dot−dashed line) UMP−DID cross term. Intensities are given on an arbitrary scale.

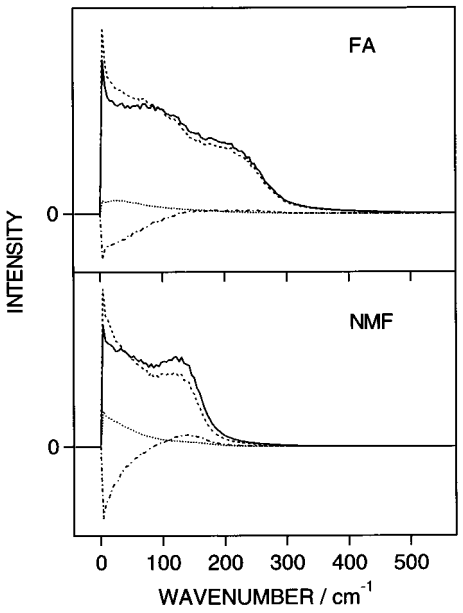

Figure 4. Fourier transform of the optical Kerr effect responses of liquid formamide (FA) and *N*-methylformamide (NMF) shown in Figure 3.

11] arising from the librational motions of molecules. The contribution of librational motions dominates the short-time profile of OKE responses also in the case of liquid acetonitrile,[19] but the other terms are important in the case of liquid water.[47] It may be said that the dominance of the librational term in the short-time profile of OKE response is characteristic of liquids with substantial anisotropy in (and with only small effects of the DID term of) molecular polarizability tensors. By contrast, the contribution of the DID term [$S^{DID}(t)$] decays slowly without significant oscillations, and most of it is canceled by the contribution of the cross term [$S^{U-D}(t)$]. The cross term is also negative in the case of liquid acetonitrile[19] but is positive in the case of liquid water.[47]

The spectral components of the OKE responses are clearly seen by taking the Fourier transform, as shown in Figure 4. These spectra are different from the Raman spectra shown in Figure 1 because of the existence of the Bose factor $\{1 - \exp[-hc\nu/(kT)]\}$ in the latter as given in eq 1. It is noted that, especially in the case of liquid NMF, the interaction-induced terms [$S^{DID}(t) + S^{U-D}(t)$] enhance the librational components appearing in the region above 100 cm^{-1} but suppress the long-time (low-frequency) components describing rotational diffusion.

Keyes et al.[28] have shown that, when the librational components of the polarizability correlation function relax more slowly than the interaction-induced component, the cross term is negative and has time dependence similar to the slower components. Negative cross terms are also seen for liquids without clear separation of the time scales of librational and interaction-induced components.[31,44] Ladanyi and Keyes[29] have suggested, by using a dielectric continuum model, that the anisotropy of molecular polarizability is reduced in the liquid phase by intermolecular interactions. In the cases of liquid FA and NMF, the situation is more complicated, since the cross term redistributes some Raman intensities from the 0−100 cm^{-1} region to the 100−200 cm^{-1} region as shown in Figures 2 and 4. In fact, the oscillation of the cross term in the OKE response shown in Figure 3 is in phase with that of the UMP term. The anisotropy of molecular polarizability is enlarged to some extent by the DID mechanism in the cases of both liquid FA and NMF. In this sense, the intensities arising from librational motions are enhanced by intermolecular interactions.

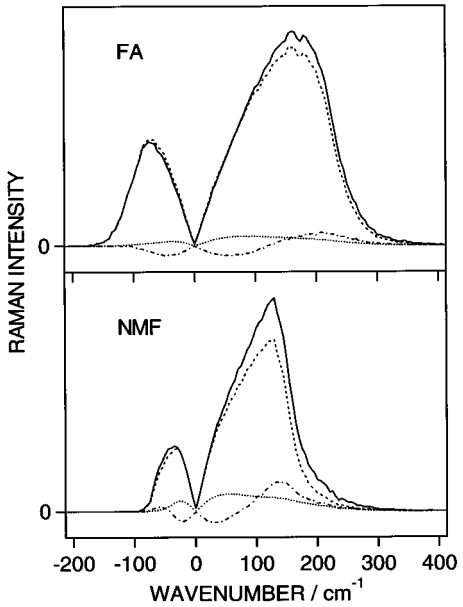

Figure 5. Raman spectra of liquid formamide (FA) and *N*-methylformamide (NMF) calculated by the INM method: (solid line) total profile; (dashed line) unperturbed molecular polarizability (UMP) component; (dotted line) dipole-induced dipole (DID) component; (dot−dashed line) UMP−DID cross term. Intensities are given on an arbitrary scale. As is usually done, imaginary wavenumber modes are plotted on the negative wavenumber side.

B. INM Analyses of Raman Spectra and Densities of States. The Raman spectra of liquid FA and NMF calculated by the INM method are shown in Figure 5. As usually done, imaginary wavenumber modes are plotted on the negative wavenumber side. Similar to the Raman spectra directly obtained from MD simulations shown in Figure 2, a strong Raman band extends to the region above 200 cm^{-1} in the case of liquid FA but is limited to the region below 150 cm^{-1} in the case of liquid

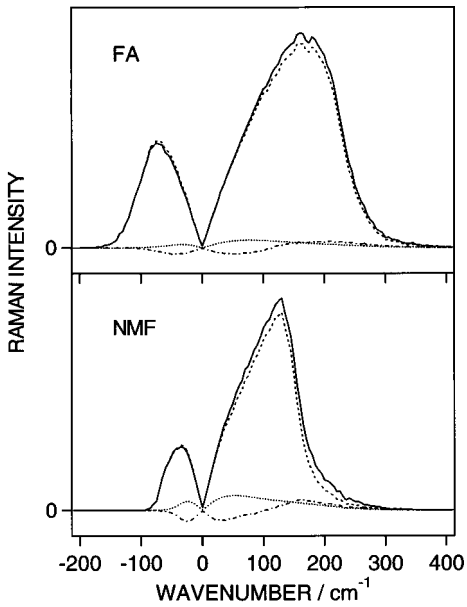

Figure 6. Raman spectra of liquid formamide (FA) and *N*-methylformamide (NMF) calculated by the INM method: (solid line) total profile; (dashed line) librational component; (dotted line) translational component; (dot−dashed line) librational−translational cross term.

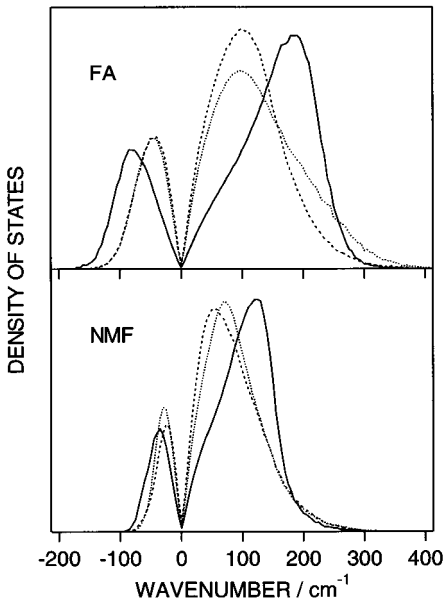

Figure 7. Density of states for librations around molecular principal axes of inertia calculated for liquid formamide (FA) and *N*-methylformamide (NMF): (dotted line) around the *x* axis (the out-of-plane axis); (dashed line) around the *y* axis (the shorter in-plane axis); (solid line) around the *z* axis (the longer in-plane axis).

NMF. There are some differences in the spectral profiles between the two sets of spectra (Figure 2 vs 5), aside from the appearance of imaginary wavenumber bands in Figure 5. However, it is most reasonable to consider that these two sets of spectra are sufficiently similar to each other so that effects of anharmonicity of the liquid dynamics on the Raman spectral features do not appear to be very large.

Each of the Raman spectra shown in Figure 5 is decomposed into the UMP, DID, and their cross term according to eqs 20−22. It is easily recognized that the similarity between Figures 2 and 5 persists into the form of the decomposed spectra; the UMP term dominates the whole wavenumber range (especially for liquid FA), the DID term gives rise to some intensities in the 0−100 cm^{-1} region, and the cross term cancels this contribution of the DID term and gives rise to positive Raman intensities in the region above 100 cm^{-1} (especially for liquid NMF).

All the above results suggest the validity of the INM approach for calculating the low-wavenumber Raman spectra of liquid FA and NMF and for examining the factors that determine the main features of these spectra.

As explained in section 2.B, Raman spectra calculated by the INM method may be decomposed in a different way into contributions of the translational and librational motions of molecules and their cross term according to eqs 27−29. The results are shown in Figure 6. It is seen that the librational component matches the total spectral profile more closely than the UMP component shown in Figure 2, especially in the case of liquid NMF. The magnitudes of the translational component and the translational−librational cross term are smaller than those of the DID component and the UMP−DID cross term. In other words, the librational components of the Raman intensities are enhanced to some extent by intermolecular interactions. However, according to the decomposition scheme used in Figure 5, this enhancement mainly originates from the UMP−DID cross term. This result is in contrast to that obtained for liquid acetonitrile, where the librational component is reduced to some extent by intermolecular interactions.[19]

To examine the nature of the librational motions that give rise to the Raman spectral features, the density of states is calculated for the libration around each molecular axis as

$$D_k^{\mathrm{lib}}(\nu) = \sum_{n=1}^{6N} \delta(\nu - \nu_n) \sum_{q=1}^{N} \left(\frac{\partial w_{kq}}{\partial Q_n} \right)^2 \qquad (30)$$

for $k = x, y, z$. The result is shown in Figure 7. It is seen that the librations around the *z* axis (shown in Figure 1) contribute most to the modes at ∼190 cm^{-1} in the case of liquid FA and at ∼120 cm^{-1} in the case of liquid NMF. These wavenumbers are almost the same as the peak wavenumbers of the Raman spectra shown in Figure 6. It is therefore considered that the difference in the wavenumber positions of the librations around the *z* axis is the main reason for the difference in the spectral features between liquid FA and NMF. The librations around the *x* and *y* axes contribute to the modes in a lower-wavenumber region, peaked at ∼100 cm^{-1} in the case of liquid FA and at 55−70 cm^{-1} in the case of liquid NMF. These librational motions generate some Raman intensities on the low-wavenumber side of the Raman bands shown in Figure 6. The wavenumber region with a larger density of states of the translational motions exists on an even lower-wavenumber side (55−70 cm^{-1} for liquid FA and 30−40 cm^{-1} for liquid NMF), although the tail extends to the wavenumber region above 200 cm^{-1} (liquid FA) or 150 cm^{-1} (liquid NMF). Such a difference in the wavenumber region between the translational and librational motions suggests that the mode coupling theory,[48−50] which treats the dynamics of liquid density fluctuations (arising from translational motions), cannot be applied for examining Raman spectra at least in the case of liquid FA and NMF.

Taking into account the results of the ab initio MO calculations in our previous study,[22] it is most reasonable to consider that the difference in the wavenumber positions of the librations around the *z* axis between liquid FA and NMF mainly arises from the existence of a hydrogen bond to the NH group on the cis position to the C═O group in FA, which resists the libration around the *z* axis, and the absence of this type of hydrogen bond in NMF. In other words, the difference in the Raman spectral profiles between the two liquids reflects the difference

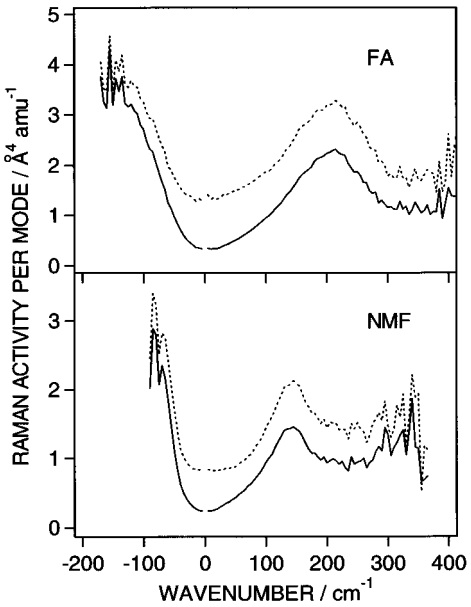

Figure 8. Raman activities generated per normal mode calculated for liquid formamide (FA) and *N*-methylformamide (NMF): (solid line) total profile (eq 31); (dashed line) librational component (eq 32).

in the dimensionality of hydrogen bonding in the liquids: two-dimensional in liquid FA and one-dimensional in liquid NMF. It has also been shown in ref 22 that the Raman intensities arising from the librations in the out-of-plane directions (around the *y* and *z* axes) are intrinsically larger than those arising from the other types of motions, and the effects of intermolecular interactions on these Raman intensities are small. These results are consistent with those obtained in the present study.

To examine the calculated Raman intensities more quantitatively, the Raman activities generated per normal mode, expressed as

$$A(\nu) = R(\nu)/D(\nu) \tag{31}$$

$$A^{\mathrm{lib}}(\nu) = R^{\mathrm{lib}}(\nu)/D^{\mathrm{lib}}(\nu) \tag{32}$$

are calculated,[51] where $D(\nu)$ is the total density of states and $D^{\mathrm{lib}}(\nu)$ is its librational component $[=D_x^{\mathrm{lib}}(\nu) + D_y^{\mathrm{lib}}(\nu) + D_z^{\mathrm{lib}}(\nu)]$. The result is shown in Figure 8. It is noted that the peak wavenumbers of $A(\nu)$ and $A^{\mathrm{lib}}(\nu)$ in the real wavenumber region almost coincide with those of the Raman spectra shown in Figure 6. This is because the Raman spectral profiles are mainly determined by the contribution from the librations around the *z* axis, and the Raman intensities arising from the librations around the *z* axis are intrinsically stronger than those arising from the other types of motions. The peak value of $A^{\mathrm{lib}}(\nu)$ is 3.28 Å^4 amu^{-1} (at 215 cm^{-1}) in the case of liquid FA and 2.13 Å^4 amu^{-1} (at 145 cm^{-1}) in the case of liquid NMF. These values are nearly the same as the intrinsic Raman activities of the librations around the *z* axis (generated by simple rotation of the unperturbed molecular polarizability tensor) calculated by the ab initio MO method in our previous study,[22] which are 2.878 Å^4 amu^{-1} (FA) and 1.866 Å^4 amu^{-1} (NMF). The peak value of $A(\nu)$ is smaller to some extent than that of $A^{\mathrm{lib}}(\nu)$ because the tail of the density of states of the translational motions extends to the wavenumber region above 200 cm^{-1} (liquid FA) or 150 cm^{-1} (liquid NMF). In contrast, the value of $A(\nu)$ in the 0−50 cm^{-1} region is smaller by a factor of 3 or 4 than that of $A^{\mathrm{lib}}(\nu)$ because the normal modes in this wavenumber region mainly involve translational motions of molecules.

4. Conclusions

The conclusions obtained in the present study may be summarized as follows. (1) The Raman spectra of liquid FA and NMF calculated by either the MD or INM method are in reasonable agreement with those observed in previous studies.[23,24] It may be said that the effects of anharmonicity of the liquid dynamics on the Raman spectral features are not very large. The calculated OKE responses are also in agreement with those observed in refs 8 and 9. It is considered that the main factors that determine the features of these optical signals are involved in the present calculations. (2) The Raman spectral features and the oscillatory profiles of the OKE responses are mainly explained by the contribution of the UMP term, in which only librational motions are involved. In other words, the anisotropy of the unperturbed molecular polarizability tensor $[\boldsymbol{\alpha}_p^{(0)}]$ is large enough so that the time derivative of $C(t)$ arising from simple libration of $\boldsymbol{\alpha}_p^{(0)}$ explains the main part of the above optical responses. Especially in the case of liquid NMF, the Raman intensities arising from librational motions are enhanced to some extent by the contribution of the UMP−DID cross term. (3) The DID term gives rise to small Raman intensities in a lower-wavenumber region than the UMP term and to slowly decaying profiles in the OKE responses. However, these are canceled by the contribution of the UMP−DID cross term. (4) The marked difference between the Raman spectra of liquid FA and NMF arises from a difference in the librations of molecules around the *z* axis. The difference is related to the dimensionality of hydrogen bonding in the liquids: two-dimensional in liquid FA and one-dimensional in liquid NMF. (5) The results of the present calculations are consistent with those obtained in our previous study[22] from ab initio MO calculations carried out for clusters of FA and NMF. As shown above, the most prominent difference in the Raman spectral features between the two liquids is related to the difference in the local liquid dynamics, the properties of which do not change very much by the effects of anharmonicity and structural disorder.

It is suggested that the features of the optical signals of liquid FA and NMF may be regarded as characteristic of strongly interacting liquids with substantial anisotropy in molecular polarizability tensors. Comparison of the present results with those obtained for other liquids in previous studies indicates that the properties of liquid dynamics giving rise to main features of optical signals are different for different types of liquids. Studies of a larger number of liquid systems may be needed to clarify this point.

References and Notes

(1) Faurskov Nielsen, O. *Ann. Rep. Prog. Chem., Sect. C: Phys. Chem.* **1993**, *90*, 3; **1996**, *93*, 57.
(2) Perova, T. S. *Adv. Chem. Phys.* **1994**, *87*, 427.
(3) McMorrow, D.; Lotshaw, W. T.; Kenney-Wallace, G. A. *IEEE J. Quantum Electron.* **1988**, *24*, 443.
(4) McMorrow, D.; Lotshaw, W. T. *J. Phys. Chem.* **1991**, *95*, 10395.
(5) Geiger, L. C.; Ladanyi, B. M. *Chem. Phys. Lett.* **1989**, *159*, 413.
(6) Cho, M.; Rosenthal, S. J.; Scherer, N. F.; Ziegler, L. D.; Fleming, G. R. *J. Chem. Phys.* **1992**, *96*, 5033.
(7) Wynne, K.; Galli, C.; Hochstrasser, R. M. *Chem. Phys. Lett.* **1992**, *193*, 17.
(8) Chang, Y. J.; Castner, E. W., Jr. *J. Chem. Phys.* **1993**, *99*, 113.
(9) Chang, Y. J.; Castner, E. W., Jr. *J. Phys. Chem.* **1994**, *98*, 9712.
(10) Deuel, H. P.; Cong, P.; Simon, J. D. *J. Phys. Chem.* **1994**, *98*, 12600.
(11) Ruhman, S.; Kohler, B.; Joly, A. G.; Nelson, K. A. *Chem. Phys. Lett.* **1987**, *141*, 16. Ruhman, S.; Kohler, B.; Joly, A. G.; Nelson, K. A. *IEEE J. Quantum Electron.* **1988**, *24*, 470.
(12) Tanimura, Y.; Mukamel, S. *J. Chem. Phys.* **1993**, *99*, 9496.
(13) Tominaga, K.; Yoshihara, K. *Phys. Rev. Lett.* **1995**, *74*, 3061.
(14) Steffen, T.; Duppen, K. *Phys. Rev. Lett.* **1996**, *76*, 1224.

(15) Tokmakoff, A.; Fleming, G. R. *J. Chem. Phys.* **1997**, *106*, 2569.
(16) Mukamel, S. *Principles of Nonlinear Optical Spectroscopy*; Oxford University Press: New York, 1995.
(17) Maroncelli, M.; Kumar, V. P.; Papazyan, A. *J. Phys. Chem.* **1993**, *97*, 13.
(18) Raineri, F. O.; Friedman, H. L. *J. Chem. Phys.* **1994**, *101*, 6111.
(19) Ladanyi, B. M.; Klein, S. *J. Chem. Phys.* **1996**, *105*, 1552.
(20) Smith, N. A.; Lin, S.; Meech, S. R.; Shirota, H.; Yoshihara, K. *J. Phys. Chem. A* **1997**, *101*, 9578.
(21) Smith, N. A.; Meech, S. R. *Faraday Discuss.* **1997**, *108*, 35.
(22) Torii, H.; Tasumi, M. *Int. J. Quantum Chem.* **1998**, *70*, 241.
(23) Faurskov Nielsen, O.; Lund, P.-A.; Praestgaard, E. *J. Chem. Phys.* **1982**, *77*, 3878.
(24) Faurskov Nielsen, O.; Christensen, D. H.; Have Rasmussen, O. *J. Mol. Struct.* **1991**, *242*, 273.
(25) Torii, H.; Tasumi, M. *J. Phys. Chem. B* **1998**, *102*, 315.
(26) Keyes, T. *J. Phys. Chem. A* **1997**, *101*, 2921.
(27) Stratt, R. M. *Acc. Chem. Res.* **1995**, *28*, 201.
(28) Keyes, T.; Kivelson, D.; McTague, J. P. *J. Chem. Phys.* **1971**, *55*, 4096.
(29) Ladanyi, B. M.; Keyes, T. *Mol. Phys.* **1977**, *33*, 1063.
(30) Kivelson, D.; Madden, P. A. *Annu. Rev. Phys. Chem.* **1980**, *31*, 523.
(31) Frenkel, D.; McTague, J. P. *J. Chem. Phys.* **1980**, *72*, 2801.
(32) Ladanyi, B. M. *J. Chem. Phys.* **1983**, *78*, 2189.
(33) Madden, P. A.; Tildesley, D. J. *Mol. Phys.* **1985**, *55*, 969.
(34) Jorgensen, W. L.; Swenson, C. J. *J. Am. Chem. Soc.* **1985**, *107*, 569.
(35) Evans, D. J. *Mol. Phys.* **1977**, *34*, 317.
(36) Allen, M. P.; Tildesley, D. J. *Computer Simulation of Liquids*; Oxford University Press: Oxford, 1989.
(37) Marcus, Y. *Introduction to Liquid State Chemistry*; Wiley: London, 1977.
(38) The prefactor $8\pi\nu/(kT)$ is included on the right-hand side of eq 1 so that the definition of $R(\nu)$ is consistent between sections 2.A and 2.B.
(39) Murry, R. L.; Fourkas, J. T.; Keyes, T. *J. Chem. Phys.* **1998**, *109*, 2814.
(40) Frisch, M. J.; Trucks, G. W.; Schlegel, H. B.; Gill, P. M. W.; Johnson, B. G.; Robb, M. A.; Cheeseman, J. R.; Keith, T.; Petersson, G. A.; Montgomery, J. A.; Raghavachari, K.; Al-Laham, M. A.; Zakrzewski, V. G.; Ortiz, J. V.; Foresman, J. B.; Cioslowski, J.; Stefanov, B. B.; Nanayakkara, A.; Challacombe, M.; Peng, C. Y.; Ayala, P. Y.; Chen, W.; Wong, M. W.; Andres, J. L.; Replogle, E. S.; Gomperts, R.; Martin, R. L.; Fox, D. J.; Binkley, J. S.; Defrees, D. J.; Baker, J.; Stewart, J. P.; Head-Gordon, M.; Gonzalez, C.; Pople, J. A. *Gaussian 94*; Gaussian, Inc.: Pittsburgh, PA, 1995.
(41) For technical reasons, the iterations were done by using translational coordinates without the weight of atomic masses. The polarizability derivatives thus obtained were transformed to those in the mass-weighted coordinate system.
(42) Bertie, J. E.; Eysel, H. H.; Permann, D. N. S.; Kalantar, D. H. *J. Raman Spectrosc.* **1985**, *16*, 137.
(43) In our previous studies (refs 22 and 25), low-wavenumber Raman spectra calculated as polarizability derivatives squared multiplied by the Bose factor were presented. The spectra obtained from eqs 20−22 and 27−29 in the present study are in a form that can be directly compared with observed Raman spectra in the so-called $R(\nu)$ representation.
(44) Geiger, L. C.; Ladanyi, B. M. *J. Chem. Phys.* **1987**, *87*, 191; **1989**, *91*, 2764.
(45) Stassen, H.; Steele, W. A. *J. Chem. Phys.* **1995**, *103*, 4408.
(46) Edwards, D. M. F.; Madden, P. A. *Mol. Phys.* **1984**, *51*, 1163.
(47) Saito, S.; Ohmine, I. *J. Chem. Phys.* **1997**, *106*, 4889.
(48) Götze, W. In *Liquids, Freezing and Glass Transition*; Hansen, J. P., Levesque, D., Zinn-Justin, J., Eds.; North-Holland: Amsterdam, 1991; p 287.
(49) Götze, W.; Sjögren, L. *Rep. Prog. Phys.* **1992**, *55*, 241.
(50) Cummins, H. Z.; Li, G.; Du, W.; Pick, R. M.; Dreyfus, C. *Phys. Rev. E* **1996**, *53*, 896.
(51) To make the values of $A(\nu)$ and $A^{\mathrm{lib}}(\nu)$ quantitative, the Raman intensities [$R(\nu)$ and $R^{\mathrm{lib}}(\nu)$] calculated as given in section 2.B are corrected for the contribution of the anisotropy in the diagonal terms of the Raman tensors.